Structural dynamics of hydrogen bonded methanol oligomers: Vibrational transient hole burning studies of spectral diffusion

I. R. Piletic, K. J. Gaffney, and M. D. Fayer
Department of Chemistry, Stanford University, Stanford, California 94305

(Received 5 February 2003; accepted 4 April 2003)

Frequency resolved pump-probe experiments have been conducted on the deuterated hydroxyl stretch of methanol-*d* in a solution containing 0.8% methanol-*d*/23% methanol-*h* in carbon tetrachloride. Methanol-*d* molecules that both donate and receive hydrogen bonds have an inhomogeneously broadened hydroxyl stretch absorption line centered at 2487 cm^{-1}. With a laser tuned to 2513 cm^{-1}, the high-frequency side of the absorption spectrum is excited. The equilibration of the excited state peak and the ground-state hole results in the time-dependent shift in the frequency of the signal, which is used to monitor the dynamics of spectral diffusion. Model calculations were conducted to address the influence of spectral diffusion in the ground and excited states on the experimental observables when the vibrational lifetime is comparable to the spectral diffusion time. The model calculations illustrate the influence on the signal of absorbers in the ground state that have relaxed from the excited state. This aspect of the problem has not been addressed in previous descriptions of frequency resolved pump-probe spectroscopy. The calculations were used to fit the time-dependent peak maximum, resulting in a bi-exponential frequency–frequency correlation function, with a fast time constant of roughly 0.1 ps and a slower time constant of 1.6 ± 0.3 ps. The observed dynamics have been compared with the predictions of dielectric continuum theory. The inability of a simple dielectric continuum theory to predict the observed spectral diffusion dynamics suggests that these dynamics do not result from the long-wavelength, collective orientational relaxation of the solvent. Instead the dynamics are attributed to fluctuations in the local hydrogen bond network, which is consistent with recent molecular-dynamics simulations of vibrational transient hole burning in water. © *2003 American Institute of Physics.* [DOI: 10.1063/1.1578058]

I. INTRODUCTION

The liquid state is characterized by macroscopic disorder. At a given instant in time, a large distribution of local solvent configurations exists. The continuous fluctuation of local structures also characterizes the liquid state. The microscopic dynamics that determine the rates of these fluctuations determine how quickly the instantaneous distribution of molecular scale solvent structures interconvert. Given enough time each solvent molecule will sample all statistically significant configurations. On this time scale the solvent behaves ergodically, with each solvent molecule sampling all of the local environments present in the macroscopic liquid.

The present study addresses the characterization of these dynamics in a hydrogen-bonded liquid. Two features of associated liquids have been postulated to be of prominent importance in the determination of solvent and solvation dynamics: the continuous rupture and reformation of hydrogen bonds[1,2] and the orientational relaxation of the molecular dipoles present in associated liquids.[3–9] While these two processes cannot be rigorously viewed as entirely separate dynamical events,[10] they do accentuate different aspects of the dynamics in liquids. Hydrogen bond length fluctuations principally involve hindered translations and translational diffusion, while orientation relaxation mainly involves hindered rotations and rotational diffusion.

Identifying the relative importance of hydrogen bond length and orientational relaxation dynamics has directed our frequency and time resolved studies of the deuterated hydroxyl stretch of methanol-*d* in an isotopically mixed solution of methanol dissolved in carbon tetrachloride.[11–13] The first step involved the measurement of the hydroxyl stretch vibrational anisotropy decay (orientational relaxation), which has been addressed in detail in a previous publication.[13] The anisotropy decay of the deuterated hydroxyl stretch of methanol-*d* in isotopically mixed 0.8 mol % methanol-*d*/23 mol % methanol-*h* in CCl_4 decays bi-exponentially. The bi-exponential decay occurs with time constants of 1.7 ± 0.7 ps and 17 ± 3 ps, with the fast component accounting for $60 \pm 10\%$ of the relaxation. The bi-exponential anisotropy decay has been analyzed with a restricted orientational diffusion model[14,15] that involves fast orientational diffusion within a cone of semiangle $\theta_c = 45 \pm 5°$, followed by slower, full orientational relaxation.

Many theories of solvation dynamics in dipolar liquids have concluded that the orientational relaxation dynamics of the solvent is the dominant contributor to spectral diffusion.[3–9] As a means of investigating the importance of solvent orientational relaxation in the spectral diffusion dynamics of the hydroxyl stretch of methanol-*d*, we have used the previously published experimental orientational relaxation dynamics[13] and a simple formulation of dielectric con-

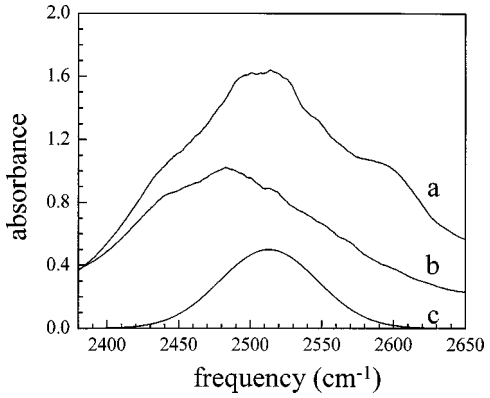

FIG. 1. Absorption spectra of (a) 0.8% methanol-*d*/23% methanol-*h* in CCl_4, (b) 0.8% methanol-*d*/23% methanol-*h* in CCl_4 with background subtraction of methanol-*h* and CCl_4. (c) Gaussian fit of the laser spectrum of the pump and probe pulses.

tinuum theory[8,9] to predict the time scales of dielectric relaxation driven spectral diffusion.

The second experimental step involved measuring the spectral diffusion dynamics of the methanol-*d* hydroxyl stretch with transient hole burning spectroscopy. Transient hole burning provides an effective technique for the investigation of spectral diffusion.[2,16–19] When the laser bandwidth is narrower than an inhomogeneously broadened absorption linewidth, a subpopulation of molecules is excited. Fluctuations in the hydroxyl stretch environment and structural relaxation of the hydrogen bonding network can result in time-dependent changes in the hydroxyl stretch absorption frequency of a methanol-*d* molecule. These spectral dynamics, termed spectral diffusion, will appear as time-dependent changes in the frequency maximum and width in the frequency resolved pump-probe signal. The time-dependent variations in the signal provide spectroscopically measurable manifestations of structural relaxation in methanol-*d* dissolved in CCl_4.

For the concentrated methanol in carbon tetrachloride solutions used in the present study, hydrogen bonded oligomers, composed of chains and rings, are the dominant species found in solution.[20,21] The frequency and width of the hydroxyl stretch absorption band depends strongly on the number of hydrogen bonds formed, making the hydroxyl stretch a sensitive probe of hydrogen bonding in solution. Figure 1 shows the infrared (IR) absorption spectra of the solution with (a) and without (b) the background. The background-free spectrum was obtained by subtracting the spectrum of pure methanol-*h* in CCl_4 from the spectrum with methanol-*d*. Two combination bands of methanol-*h* appear in this spectral region[22] although these will not affect the pump-probe signal to a significant extent as discussed in Sec. III. Methanol molecules that both accept and donate hydrogen bonds in oligomer chains and rings represent the dominant configuration in liquid methanol and at high methanol concentrations in CCl_4.[20,21] These methanol-*d* molecules, referred to as δ, have an absorption peak at $\sim$2487 cm^{-1}. The shape of the spectrum can be approximated as a Gaussian with a full width at half maximum (FWHM) of $\sim$130 cm^{-1} [see Fig. 1(b)]. The shoulder occurring at lower frequencies has been assigned to a methyl rock overtone Fermi resonance.[22]

The Gaussian width of the δ band exceeds the 90 cm^{-1} FWHM of the excitation laser pulses used in the experiments, making transient hole burning possible. The extent of spectral diffusion was determined by frequency resolving the probe pulse. The time-dependent variations in the pump-probe signal spectrum following pump excitation to the high-frequency side of the δ absorption at 2513 cm^{-1} makes it possible to directly monitor spectral diffusion. The peak of the ground state bleach spectrally diffuses to $\sim$2484 cm^{-1}, very close to the δ band absorption maximum at $\sim$2487 cm^{-1}. The diffusion occurs on two time scales of $\sim$0.1 ps and 1.6 ± 0.3 ps with the two components having roughly equal amplitudes. The time constant for the faster spectral diffusion process possesses significant uncertainty. However, the amplitude of the process can be accurately determined because the initial and final peak maxima can be accurately measured, as can the amplitude of the slower diffusion process.

To extract the spectral diffusion dynamics from the transient hole burning data, we constructed a model for frequency resolved pump-probe spectroscopy that includes the possibility that different time evolution occurs in the ground and excited states. These potential differences present a challenge in developing a model calculation. When the excited state decays to the ground state, the relaxation will occur vertically relative to the lower frequency modes of the solvent that give rise to spectral diffusion.[19] If the dynamics in the excited state differ from those in the ground state, the relaxed molecules will be characterized by a different absorption than the ground-state bleach and will undergo spectral diffusion as well. We have constructed a model that includes these relaxed molecules, which are antiholes because they provide a vibrational ground-state signal with a sign opposite that of the ground-state hole. A series of model calculations have been performed to clarify the influence of antiholes on the frequency resolved pump-probe signal, because previous models have not included this aspect of the signal.[17,19,23] The calculations demonstrate that antiholes make a significant contribution to the signal when the dynamics on the ground- and excited-state potential differ and the excited-state decay and spectral diffusion occur with similar time constants.

The measured spectral diffusion dynamics have been compared to dielectric continuum predictions based on the hydroxyl stretch orientational relaxation data measured previously.[8,9,13] As will be discussed in Sec. V, the predictions are not in accord with the observed spectral diffusion data, indicating that orientational relaxation of the solvent molecules does not determine the rate of spectral diffusion. Comparison of the time scales measured with transient hole burning and molecular-dynamics simulations of hydrogen bond lifetimes in methanol–carbon tetrachloride solutions,[21] as well as simulations of vibrational transient hole burning in water,[24] support the conclusion that the diffusion dynamics measured experimentally result from local fluctuations in the hydrogen bond network with the slower 1.6 ps relaxation

reflecting the lifetime of a hydrogen bond in a concentrated methanol solution.[21]

II. EXPERIMENTAL PROCEDURES

Deuterated methanol-*d* (Aldrich, 99.5+at.%), protonated methanol-*h* (J. T. Baker, spectroscopic grade), and carbon tetrachloride (Aldrich, HPLC grade) were used as received. Methanol-*d* has a deuterated hydroxyl group and protonated methyl group. We conducted experiments on a 0.8 mol% methanol-*d*/23 mol% methanol-*h* in the CCl_4 sample. Spectroscopic measurements used home-built copper cells with CaF_2 windows. A 1-mm Teflon spacer yielded an absorbance of ~1.7 at the peak of the absorption at ~2500 cm^{-1}. In these sample cells, the solution came in contact only with the CaF_2 and Teflon because metals, such as copper, catalyze the decomposition of alcohols in CCl_4 solution.[25]

The laser system used in these experiments consists of a home-built Ti:sapphire oscillator and regenerative amplifier whose output pumps a three-stage optical parametric amplifier (OPA) designed and built in-house to produce tunable midinfrared light with controlled pulse duration (spectral bandwidth). A bandwidth limiting slit in the stretcher determines the bandwidth of the amplified seed pulse and provides control of the IR pulse duration. The IR output is 1–2 μJ per pulse centered at 2513 cm^{-1}. The IR pulse duration was measured by autocorrelation. The pulses have Gaussian profiles in time and frequency with FWHM of 215 fs in time and 90 cm^{-1} in frequency, providing a time–bandwidth product 1.3 times the transform limit of 0.44.

The mid-IR pulses are split into pump (90%) and probe (10%) beams that traverse different paths before crossing in the sample. The pump beam is chopped at 500 Hz and directed along a variable path length delay line. A ZnSe Brewster-plate polarizer is used to set the probe beam polarization. We used a probe polarization parallel to the pump polarization for all of the experiments in this paper. We dispersed the probe beam in a monochromator set to ~3 cm^{-1} resolution. By scanning the frequency of the monochromator and the time delay between the pump and probe pulses, the time evolution of the pump-probe signal could be monitored as a function of frequency with high spectral resolution. The frequency resolved data used liquid-nitrogen-cooled InSb and Mercury Cadmium Telluride detectors for the signal and reference, respectively. We process the detector outputs in gated integrators, divide the signal by the reference in an analog processor, and input the processor output into a lock-in amplifier. A computer controls a stepper motor delay line and collects the output of the lock-in with an analog to digital board. Frequency resolved data were collected by scanning the monochromator for a number of time delays.

III. FREQUENCY RESOLVED PUMP-PROBE EXPERIMENTAL RESULTS

We conducted one color frequency resolved pump-probe experiments on a 0.8% methanol-*d*/23% methanol-*h* in CCl_4 solution by dispersing the pump-probe signal in a monochromator. This differs from the vibrational transient hole burning experiments conducted by Gale *et al.*,[2] Laenen *et al.*,[16] and Woutersen and Bakker,[17] where the frequency integrated signal as a function of probe frequency for a fixed pump frequency provides the frequency resolution. The advantage of collecting frequency resolved data with a monochromator, as opposed to performing two color experiments, is the higher frequency resolution. The disadvantage of one color experiments is the narrower frequency range over which spectral dynamics can be observed. Any spectral evolution approaching the tails of the laser spectrum will produce nonnegligible errors due to the low laser intensity, limiting our study to a frequency range from 2420 to 2575 cm^{-1}.

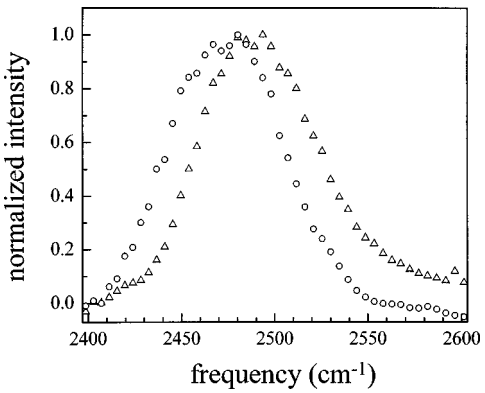

FIG. 2. Normalized pump-probe spectra at delay times $t=0.3$ ps (△) and $t=6$ ps (○). The signal shifts towards lower frequency because of spectral diffusion.

The Gaussian laser spectrum centered at 2513 cm^{-1} is blueshifted relative to the maximum of the δ band in the background subtracted IR spectrum. This laser spectrum creates a hole narrower than the absorption band and displaced from the ground-state absorption maximum. Spectral diffusion will cause the hole to shift to the absorption maximum and broaden to the width of absorption line. Molecules in the excited state also contribute to the frequency-dependent signal via stimulated emission. The spectrum of the excited vibrational state will shift and broaden until it matches what would be the equilibrated fluorescence spectrum, which is not observable because of the negligible fluorescence quantum yield. The equilibrated fluorescence spectrum need not coincide with the ground-state absorption spectrum because of a possible Stokes shift.[17,19,26] The excited state will also absorb the probe pulse if the anharmonic shift of the 1–2 transition does not exceed the bandwidth of the laser. For the hydroxyl stretch of methanol-*d*, the anharmonicity significantly exceeds the 90 cm^{-1} FWHM of the laser spectrum, so excited-state absorption does not make a contribution to the observed signal.[27]

Figure 2 depicts normalized spectra of the pump-probe signal for time delays of 0.3 and 6 ps. Normalization emphasizes the spectral diffusion process and suppresses the influence of population dynamics on the signal, which we discussed in a previous publication.[12] A frequency-dependent lifetime, like that observed for the hydroxyl stretch of methanol-*d*,[12,27,28] may produce a time-dependent pump-probe spectrum. Previous experiments have shown that higher frequency absorbers decay more slowly, with a weak

frequency-dependent lifetime in the range where the vast majority of our signal originates.[12] The frequency dependence of the lifetime would result in a time-dependent spectral shift to higher frequency, while the experimentally observed signal shifts to lower frequency, demonstrating that the frequency-dependent lifetime does not produce the observed spectral dynamics. As clearly seen in Fig. 2, the signal shifts to lower frequency as the pump-probe delay increases. When analyzed appropriately, these spectral dynamics can be utilized to monitor the time scale for structural evolution in the solvent. Before addressing the solvent dynamics, the method of analysis is presented.

For the time-dependent spectra of the hole and the excited state stimulated emission to be extracted from the time-dependent spectra of the pump-probe signal depicted in Fig. 2, the influence of the probe spectrum must be deconvolved from the pump-probe signal spectra. As will be demonstrated, this can be achieved by dividing the pump-probe signal spectrum by the probe spectrum after it is attenuated by the wavelength dependent absorption of the sample.

We interpret the pump-probe experiment as two sequential linear absorption experiments where the sample linearly attenuates each pulse. This provides a valid interpretation of the data for pump-probe separations comparable to or larger than the ~200 fs pulse durations.[19,29] When the pump and probe pulses have significant temporal overlap, phase and amplitude gratings will make non-negligible contributions to the signal and complicate the data analysis significantly.[29] Therefore the data analysis is limited to delay $\geqslant$200 fs.

The experimental signal monitors the change in intensity (ΔI) of the probe beam with and without the pump beam as a function of pump-probe delay and probe frequency. As given by the Beer-Lambert Law, the intensity of a probe pulse in the absence of a pump pulse is

$$I_{\mathrm{NP}}(\omega)=I_0(\omega)\exp\{-\varepsilon_M(\omega)[C_{IM}(\omega)]l - \varepsilon_B(\omega)[C_{IB}(\omega)]l\}, \tag{1}$$

where the subscript NP denotes no pump, $\varepsilon_M(\omega)$ and $\varepsilon_B(\omega)$ denote the molar absorptivities of methanol-*d* and the background, respectively, $C_{IM}(\omega)$ and $C_{IB}(\omega)$ denote the initial ground-state concentrations of methanol-*d* and the background absorbers respectively, and l denotes the path length of the sample. Figure 1 demonstrates that the absorbance of the methanol-*d* hydroxyl stretch exceeds or is comparable to the background absorption. The background absorption has been associated with combination bands from the methanol-*h*.[22] These combination bands have a significant absorption because the total methanol-*h* concentration greatly exceeds the methanol-*d* concentration, even though $\varepsilon_M(\omega)\geqslant\varepsilon_B(\omega)$. This larger magnitude of ε_M leads to significant background suppression in the pump-probe spectrum, as will be demonstrated.

Having the pump pulse proceed the probe pulse changes the probe attenuation in two ways; the pump pulse places molecules in the excited state, which reduces the ground-state absorption, and the molecules placed in the excited state can be stimulated to emit photons by the probe pulse. Both processes result in a transmitted probe pulse with an increased intensity relative to the transmitted probe pulse in the absence of the pump pulse. The ground-state concentrations of the deuterated hydroxyl stretch and the background following excitation of the sample by the pump pulse can be expressed as

$$\begin{aligned} C_{GM}(\omega,t)&=C_{IM}(\omega)-\Delta C_{HM}(\omega,t),\\ C_{GB}(\omega,t)&=C_{IB}(\omega)-\Delta C_{HB}(\omega,t), \end{aligned} \tag{2}$$

with $\Delta C_{HM}(\omega,t)$ and $\Delta C_{HB}(\omega,t)$ representing the time-dependent population holes in the ground state, $C_{GM}(\omega,t)$ and $C_{GB}(\omega,t)$ representing the methanol-*d* and background populations left in the ground state following pump excitation, respectively, and $C_{IM}(\omega)$ and $C_{IB}(\omega)$ as defined above. The excited-state concentrations that give rise to stimulated emission are designated as $C_{ESM}(\omega,t)$ and $C_{ESB}(\omega,t)$ for the deuterated hydroxyl stretch and the background, respectively. The intensity of the probe pulse after the pump pulse has passed through the sample is

$$\begin{aligned} I_P(\omega,t)&=I_0(\omega)\exp[-\varepsilon_M(\omega)C_{GM}(\omega,t)l-\varepsilon_B(\omega)C_{GB}(\omega,t)l]\\ &\quad\times\exp[\varepsilon_M(\omega)C_{ESM}(\omega,t)l+\varepsilon_B(\omega)C_{ESB}(\omega,t)l]. \end{aligned} \tag{3}$$

The first exponential term is an attenuation term from molecules that absorb the probe pulse, while the second exponential term represents amplification from excited-state molecules that undergo stimulated emission. The same extinction coefficients apply in the latter term because the Einstein *B* coefficient for absorption equals the Einstein *B* coefficient for stimulated emission.[30]

A typical pump-probe experiment monitors the change in the probe intensity ΔI due to the absorption of the pump pulse. By taking the difference of the above equations the change in transmitted probe intensity equals

$$\begin{aligned} \Delta I(\omega,t)&=I_P(\omega,t)-I_{\mathrm{NP}}(\omega)\\ &=I_o(\omega)\exp\{-[\varepsilon_M(\omega)C_{IM}(\omega)+\varepsilon_B(\omega)C_{IB}(\omega)]l\}\\ &\quad\times(\exp\{\varepsilon_M(\omega)[\Delta C_{HM}(\omega,t)+C_{ESM}(\omega,t)]l\}\\ &\quad\times\exp\{\varepsilon_B(\omega)[\Delta C_{HB}(\omega,t)+C_{ESB}(\omega,t)]l\}-1). \end{aligned} \tag{4}$$

For the sample studied in the present paper, the absorbance of the hydroxyl stretch of methanol-*d* exceeds or is comparable to the background absorbance in the frequency range covered by our pulses. As a consequence, the hole and excited-state concentrations of the hydroxyl stretch of methanol-*d* exceed or equal those for the background,

$$\Delta C_{HB}(\omega,t)+C_{ESB}(\omega,t)\leqslant\Delta C_{HM}(\omega,t)+C_{ESM}(\omega,t). \tag{5}$$

Because $\varepsilon_M(\omega)\geqslant\varepsilon_B(\omega)$, the $\varepsilon_M(\omega)$ will dominate the signal, leading to the following simplification of Eq. (4):

$$\begin{aligned} \Delta I(\omega,t)&=I_{\mathrm{NP}}(\omega)(\exp\{\varepsilon_M(\omega)\\ &\quad\times[C_{HM}(\omega,t)+C_{ESM}(\omega,t)]l\}-1). \end{aligned} \tag{6}$$

In these experiments, the initial populations greatly exceed the changes in population, $C_I(\omega)\geqslant C_H(\omega,t)+C_{\mathrm{ES}}(\omega,t)$.

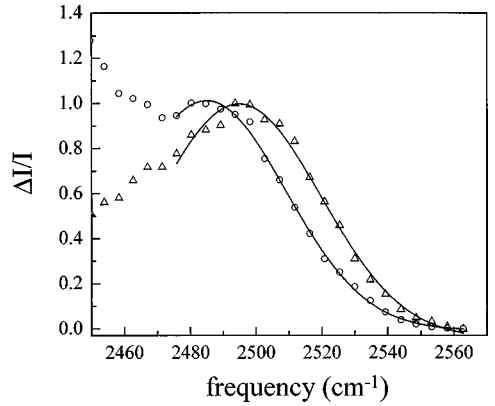

FIG. 3. Spectra of the excited-state peak and ground-state hole at delay times $t=0.3$ ps (△) and $t=6$ ps (○). The fit of each spectra to a single Gaussian provides the time-dependent peak position data in Fig. 4. The growing shoulder on the low-frequency side results from a methyl rock overtone of methanol-*d* with a slower decay than the δ methanol-*d* hydroxyl stretch. To minimize the influence of this overtone on the extracted spectral diffusion dynamics, we only fit the data from 2475 to 2560 cm^{-1}.

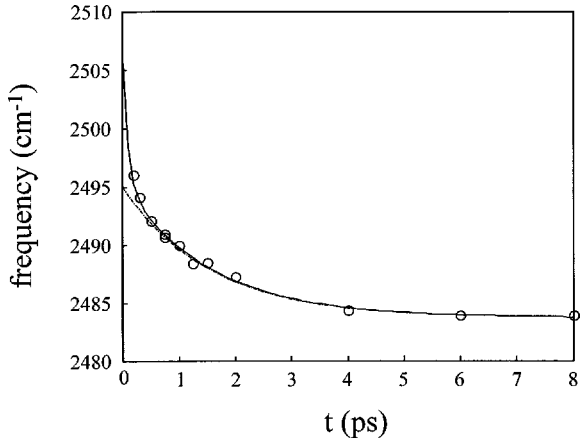

FIG. 4. A plot of the peak position of the Gaussian fit to all normalized signal spectra versus time. While a single exponential with a time constant of 1.6 ± 0.3 ps fits the data between 0.75 and 8 ps, this fit extrapolates to a time zero-frequency maximum of $\sim$2495 cm^{-1}, roughly 10 cm^{-1} too low, and cannot fit the peak positions at 0.2 and 0.3 ps. A bi-exponential with time constants of $\sim$60 fs and 1.6 ± 0.3 ps effectively fits all data, and extrapolates to a correct initial peak maximum near $\sim$2505 cm^{-1}.

This property can be exploited by Taylor expanding the exponential in the brackets and truncating the expansion after the first two terms. This produces our final expression for the pump-probe signal:

$$\Delta I(\omega,t)=I_{\mathrm{NP}}(\omega)\varepsilon_M(\omega)[\Delta C_{HM}(\omega,t)+C_{ESM}(\omega,t)]l. \tag{7}$$

Division of this signal by $I_{\mathrm{NP}}(\omega)$, the attenuated probe pulse intensity in the absence of a pump pulse, demonstrates how the spectrum of the hole and excited state can be accessed in a frequency resolved pump-probe experiment:

$$\frac{\Delta I(\omega,t)}{I_{\mathrm{NP}}(\omega)}=\varepsilon_M(\omega)[\Delta C_{HM}(\omega,t)+C_{ESM}(\omega,t)]l. \tag{8}$$

We utilized Eq. (8) to extract the combined ground-state bleach plus excited-state stimulated emission spectra shown in Fig. 3 from the pump-probe spectra shown in Fig. 2. We calculated I_{NP} by substituting the absorption spectrum, $\varepsilon_M(\omega)[C_{IM}(\omega)]l+\varepsilon_B(\omega)[C_{IB}(\omega)]l$, as measured with Fourier transform infrared (FTIR) and the laser spectrum $I_0(\omega)$ into Eq. (1). Equation (8) shows that excited-state and ground-state spectral diffusion cannot be separated in a transient hole burning experiment. The consequences of this will be discussed in the following section.

Figure 3 shows the excited-state emission plus ground-state bleach spectrum for time delays of 0.3 and 6 ps. A prevalent peak associated with the δ methanol-*d* hydroxyl stretch appears in all pump-probe spectra, which we fit to a Gaussian in the frequency range between 2475 and 2565 cm^{-1}. This peak persists for delay times much longer than the lifetime of $\tau_r\approx500$ fs because hydrogen bond dissociation following vibrational relaxation produces a persistent ground-state hole[12] which permits the measurement of spectral and orientational[13] diffusion on time scales much longer than the excited state lifetime. A peak on the lower frequency side of the δ peak due to the methyl rock overtone Fermi resonance[22] makes an increasingly significant contribution to the signal as the time delay increases. We have limited our analysis of the spectral diffusion dynamics to frequencies $\geqslant$2475 cm^{-1} to reduce the influence of this overtone absorption on the extracted dynamics. The strong similarity between the final frequency maximum of the ground-state hole, 2484 cm^{-1}, and the absorption maximum, 2487 cm^{-1}, demonstrates that the presence of the overtone has little or no effect on the peak position data we have used to monitor spectral diffusion dynamics.

We fit the ground-state bleach plus excited-state emission spectra for each delay time to a single Gaussian in the frequency range from 2475 to 2565 cm^{-1}. While the stimulated emission and ground-state bleach could each be fit with a separate Gaussian, our experimental data can be fit adequately with only a single Gaussian, as shown in Fig. 3. In principle, both the time-dependent peak position and width of the Gaussian fit can be used to describe the spectral diffusion. The time-dependent width did not provide a sensitive probe of the spectral dynamics due to the poor signal to noise in the wings of the laser spectrum and the presence of the Fermi resonance on the low-frequency side of the pump-probe spectra. As a result it will not be discussed further. Figure 4 shows the peak position versus time and a fit of the dynamics to a single exponential (broken curve) and a bi-exponential (solid curve). The peak position plot can be adequately fit to a single exponential time constant of 1.6 ps when fitting the data between 0.75 and 8 ps. Extrapolation of this fit to zero time delay results in an initial ground-state bleach plus excited-state stimulated emission peak at 2495 cm^{-1}. According to a calculation of the pump pulse attenuation by the sample with an absorption spectrum given by Fig. 1, the initial hole and excited-state spectrum should be peaked at 2507 cm^{-1}, assuming the molar absorptivity is constant across the δ band. This demonstrates that the 1.6 ps time constant does not account for a significant fraction of the shift in the peak. The fit of the data to a single exponential also misses the 200 and 300 fs peak position data points, further supporting the conclusion that spectral diffusion in

the hydroxyl stretch of methanol occurs on two time scales, the faster of which cannot be fully resolved with 200 fs pulses. The fit of data in Fig. 4 to a bi-exponential indicates that the faster component shifts with a ~60 fs time constant and has an amplitude comparable to the 1.6 ps component. A more quantitative description of this fit will be addressed in Sec. IV.

IV. MODELING PUMP-PROBE MEASUREMENTS OF SPECTRAL DIFFUSION

We constructed a model to describe the simultaneous evolution of the ground-state bleach and the excited-state emission in a generalized hole burning experiment. Several cases of spectral diffusion will be considered in order to contrast the behavior of ground and excited state evolution, because both appear in hole burning experiments. The results will then be compared with the data already presented.

In a general hole burning experiment, a pump pulse with a bandwidth smaller than the absorption width of a given spectroscopic transition generates an excited-state population and a concentration hole in the ground state. The dynamical information contained in a transient hole burning experiment resembles that contained in time resolved fluorescence (TRF).[3,5,19] TRF monitors the dynamics of excited-state spectral diffusion via the time-dependent evolution of a solvent derived Stokes shift Λ. Analysis of experimental data usually involves the construction of a Stokes shift function that contains the time-dependent peak, or first moment, of the fluorescence spectrum:

$$S_{\mathrm{ES}}(t)=\frac{\nu(t)-\nu(\infty)}{\nu(0)-\nu(\infty)}, \tag{9}$$

where the ES subscript refers to excited-state dynamics. Linear-response theory predicts that this nonequilibrium relaxation $S_{\mathrm{ES}}(t)$ will equal the normalized equilibrium solvation energy response function $C_s(t)$, when the restoring force that returns the system to equilibrium can be viewed as linear in the displacement from equilibrium caused by the electronic excitation.[19,31] In our experiments, we excite the hydroxyl stretch of methanol-*d*, which causes a small change in the length and dipole moment of the hydroxyl bond. This constitutes a much smaller perturbation than perturbations shown to result in deviations from linear response in molecular-dynamics simulations in methanol.[32] Equation (9) is equivalent to the normalized transition frequency-transition frequency correlation function $M(t)$ in the high-temperature limit:

$$M(t)=\frac{\langle\Delta\omega(0)\Delta\omega(t)\rangle}{\langle\Delta\omega^2\rangle}, \tag{10}$$

where $\Delta\omega(t)=\langle\omega_T\rangle-\omega(t)$, $\langle\omega_T\rangle$ is the average transition frequency, and $\omega(t)$ is the time-dependent transition frequency. The angle brackets refer to an ensemble average. $M(t)$ contains information about the solvent dynamics as observed through the filter of a given spectroscopic transition.

While the formalism used to describe TRF does apply to transient hole burning experiments, one primary distinction must be understood. In TRF, the signal results only from excited-state emission, while in transient hole burning both ground-state bleaching and excited-state stimulated emission contribute. When the spectrum of these two components of the transient hole burning experiment can be resolved, a $S(t)$ can be separately constructed for the excited-state peak and the ground-state hole. Because the excited state and the ground state access the same solvent dynamics, within linear-response theory these ground and excited state correlation functions should monitor the same transition frequency–transition frequency correlation function $M(t)$:

$$S_G(t)=\frac{\nu_G(t)-\nu_G(\infty)}{\nu_G(0)-\nu_G(\infty)}=M(t)=\frac{\nu_{\mathrm{ES}}(t)-\nu_{\mathrm{ES}}(\infty)}{\nu_{\mathrm{ES}}(0)-\nu_{\mathrm{ES}}(\infty)}=S_{\mathrm{ES}}(t). \tag{11}$$

Generally, the equilibrated frequency maximum for excitation $\nu_G(\infty)$ and emission $\nu_{\mathrm{ES}}(\infty)$ will differ by the Stokes shift, even though they have the same value at time zero. Unless the fluorescence and absorption spectra are coincident, the ground and excited state contributions will move with different effective rates even though they experience the same solvation dynamics within linear-response approximations.

After calculating the ground-state bleach plus stimulated emission spectra for each delay time, we fit the spectrum to a single Gaussian to obtain the peak position versus time $P_\delta(t)$, consistent with our analysis of the experimental data. The 304-fs FWHM of the cross correlation of the pump and probe pulses must be accounted for to simulate the data. Convolution of this instrument function with $P_\delta(t)$ produces the model dynamics to be compared with experiment. The model calculations allow for different time evolution in the excited and ground state potentials. These differences could arise from either a vibrational Stokes shift, $\nu_G(\infty)=\nu_{\mathrm{ES}}(\infty)+\Lambda$, or different time constants for spectral diffusion in the excited and ground state potentials. The later effect would signify the deviation from linear-response theory. Since we assume linear response holds, we do not consider the second possibility in the model calculations. Standard models of optical spectroscopy predict the excited-state emission peak maximum to be shifted to lower frequency than the ground-state bleach by an amount equal to the Stokes shift Λ.[19] For inhomogeneously broadened absorptions, such as the δ hydroxyl stretch of methanol, these standard models indicate that the magnitude of the Stokes shift can be determined from the standard deviation Δ of the Gaussian inhomogeneous width of the adsorption band,

$$\Lambda=\hbar\Delta^2/k_BT, \tag{12}$$

with $\Delta\approx 55\ \mathrm{cm}^{-1}$ and $\Lambda\approx 15\ \mathrm{cm}^{-1}$ for the δ band of methanol-*d* in CCl_4. While these models relate Δ and Λ at all temperatures, Eq. (12) only applies in the high-temperature limit.[19] Model calculations have been conducted with and without this Stokes shift.

To model the ground-state bleach plus stimulated emission spectra for different delay times, the spectrum of the ground-state bleach plus stimulated emission at $t=0$ must be determined. The combined bleach and emission spectrum is calculated by taking the difference between the laser inten-

sity before and after it passes through the sample as a function of frequency, which produces a Gaussian $t=0$ signal, peaked at 2507 cm^{-1} before convolution with the temporal instrument function. The excited-state peak and the hole are modeled as Gaussians with time-dependent peak maxima and widths for all delay times. After $t=0$, the excited-state peak and ground-state hole shift and broaden until the former equilibrates to the equilibrium fluorescence spectrum and the latter equilibrates to the equilibrium absorption spectrum. The peak positions $\nu_G(t)$ and $\nu_{ES}(t)$ are given by

$$\nu_G(t)=\nu_G(\infty)+[\nu_G(0)-\nu_G(\infty)]M(t),$$
$$\nu_{ES}(t)=\nu_{ES}(\infty)+[\nu_{ES}(0)-\nu_{ES}(\infty)]M(t). \quad (13)$$

The lifetime of the excited state is incorporated into the calculation by attenuating the excited-state population at all frequencies with the same relaxation time, $\tau_r=500$ fs. After each time step in the calculation, the excited-state peak decays generating an antihole in the ground state. This name reflects the influence of the antiholes on the signal. The hole causes a decrease in ground-state population and produces a frequency-dependent increase in the probe intensity, whereas the antihole causes an increase in the ground-state population and generates a frequency-dependent decrease in the probe intensity. As discussed in a prior publication, vibrational relaxation leads to hydrogen bond dissociation for roughly one out of five vibrationally excited molecules with a time constant of 220 fs.[12] This hydrogen bond breaking leads to a persistent ground-state hole which we utilized to monitor spectral diffusion on time scales much longer than the excited-state lifetime. In our model calculations we make the simplifying assumption that hydrogen bond breaking occurs instantaneously following vibrational relaxation.

The same $M(t)$ governs the equilibration of the antiholes and the hole to the equilibrated absorption spectrum. The frequency maximum of an antihole at the moment of excited-state decay, however, need not be the same as that of the hole, because spectral diffusion on the excited-state potential determines the initial position of the antihole on the ground-state potential. In many important limiting cases the antihole will only attenuate the hole, but in the case of different time evolution in the excited and ground state and excited-state relaxation on the same time scale as spectral diffusion, the explicit time evolution of the ground-state antiholes must be modeled, as well as the excited-state peak and the ground-state hole. While the influence of antiholes have been disregarded in descriptions of transient hole burning,[17,19,23] they have been clearly observed in persistent vibrational hole burning experiments.[33]

A series of model calculations have been conducted to demonstrate these effects. The results are displayed in Fig. 5. The parameters for the calculations are given in Table I. In each panel there are two calculations. The solid lines are for the hypothetical case in which relaxation of the excited state directly fills the hole (no antiholes) regardless of the frequency of the excited-state peak. The dashed line is for the situation in which relation of the excited-state peak is vertical, which produces antiholes. Figure 5(A) shows the calculations when there is no Stokes shift. Without a Stokes shift,

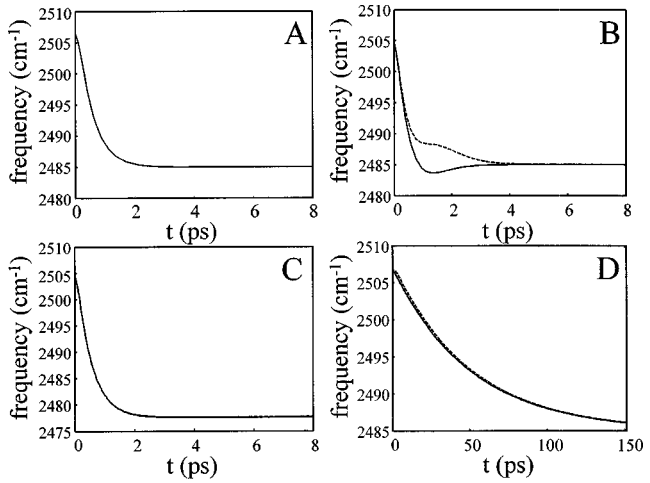

FIG. 5. Model calculations of the frequency resolved pump-probe signal. All panels contrast two situations for every delay time t: the hypothetical situation in which the excited state directly fills the ground-state hole regardless of the relative positions of the excited-state peak and the ground-state bleach (solid curves), or the excited-state decays vertically, generating an antihole with the same frequency distribution as the excited-state peak at the time of decay (dashed curve). These calculations demonstrate that antiholes only make a significant contribution to the signal when the excited state has a Stokes shift and the spectral diffusion dynamics occur on the same time scale as the vibrational decay (B). When the excited state does not have a Stokes shift (A), or spectral diffusion and vibrational decay do not occur on the same time scale, (C) and (D), antiholes do not make a significant contribution to the signal. All parameters used in these calculations appear in Table I.

antiholes simply attenuate the ground-state hole, even when $\tau_r \approx \tau_D$. The two calculations are the same because vertical relaxation produces an antihole that is not shifted with respect to the hole when there is no Stokes shift. The Stokes shift in the excited state can lead to an antihole significantly displaced from the position of the ground-state hole at the time of excited-state decay. This effect will only be observable when the spectral diffusion τ_D and excited-state relaxation τ_r occur on the same time scale. Figure 5(B) demonstrates that the antiholes significantly affect the signal for times comparable to τ_r and τ_D. Because antiholes build up on the lower frequency side of the ground-state hole, they preferentially fill the low-frequency side of the hole, and effectively slow down the peak shift (dashed curve). Distinctly different dynamics result when the unphysical situation in which the antiholes directly fill the ground-state hole (solid curve). By a time delay of $\sim$1 ps, the signal peaks at a frequency lower than that of the ground-state absorption, as a result of the excited-state Stokes shift. The signal then reverts to the time-dependent ground-state absorption spectrum as the influence of the excited-state emission decays with the

TABLE I. Parameters used in the model calculations for Fig. 5.

Figure	τ_r (ps)	τ_d (ps)	$\nu_G(\infty)$ (cm^{-1})	$\Delta_G(\infty)=\Delta_{ES}(\infty)$ (cm^{-1})	Λ (cm^{-1})
5(A)	0.5	0.5	2485	55	0
5(B)	0.5	0.5	2485	55	15
5(C)	50	0.5	2485	55	15
5(D)	0.5	50	2485	55	15

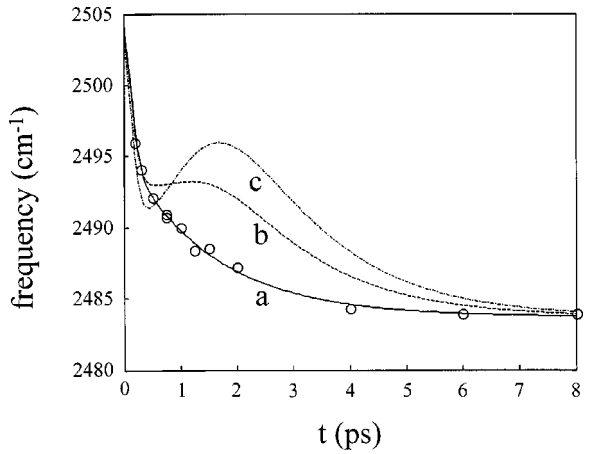

FIG. 6. A plot of the peak position versus time fit with model calculations using several different values for the Stokes shift (0 cm^{-1}: solid line; 3 cm^{-1}: dash line; 15 cm^{-1}: dash-dot line). The best fit to the experimental data does not support the presence of a vibrational Stokes shift. The parameters used in the best fit can be found in Table II.

excited-state lifetime. The tremendous differences between the simulations shown in Figs. 5(A) and 5(B) demonstrate the sensitivity of transient absorption to the Stokes shift and antiholes for spectral diffusion and vibrational decay times consistent with the hydroxyl stretch of hydrogen bonded liquids. When $\tau_r \gg \tau_D$, spectral diffusion will finish before any appreciable excited state decay has occurred. While vertical relaxation from the excited state down to the ground state will lead to an increased antihole absorption to the red of the ground-state hole, these antiholes will spectrally diffuse to the position of the ground-state hole before a detectable population of antiholes to the red edge of the ground-state hole can accumulate. Consequently, the antihole signal will not make an appreciable modification of the signal, as shown in Fig. 5(C). When $\tau_r \ll \tau_D$, no spectral diffusion will occur in the excited state, leaving the excited-state peak directly above the ground-state hole. The antihole simply attenuates the amplitude of the hole and spectral diffusion can only be monitored via the persistent ground-state hole generated by hydrogen bond dissociation following vibrational relaxation. This case appears in Fig. 5(D).

While the proper treatment of the antiholes does not appear to have been addressed in general treatments of spectral diffusion,[19] most studies have involved electronic excited states where $\tau_r \gg \tau_D$, and the antihole dynamics do not appear in the signal. Studies of hydroxyl stretch vibrational transient hole burning in hydrogen bonded liquids have also ignored the influence of the antihole signal on the observed spectral dynamics.[2,16,17,23] This could be of significance, since a vibrational Stokes shift has been observed theoretically and experimentally[17,23,26] in liquid water and $\tau_r \approx \tau_D$ for the hydroxyl stretch in water.

The model presented above has also been used to simulate the experimental time-dependent peak maximum. The data and the results of the simulations appear in Fig. 6. Two results deserve particular attention. The model requires a biexponential $M(t)$ to fit the experimental data (curve a), and the presence of a Stokes shift on the order of that expected by Eq. (12) causes a nonmonotonic shift in the signal inconsistent with our experimental data, as shown by curve c. Even with a small Stokes shift of 3 cm^{-1}, a nonmonotonic shift in the signal is observed and is depicted by curve b. The parameters used in these simulations appear in Table I. While fitting the time-dependent peak maximum indicates the absence of a Stokes shift, the shoulder due to the methyl rock overtone[22] appearing on the low-frequency side of the δ absorption in Fig. 1 complicates the analysis of the spectral dynamics at lower frequency and reduces to some extent the influence of the Stokes shift and the antihole contribution to the signal. We intend to clarify these issues with further experiments on perdeuterated methanol, which lacks this shoulder absorption.

V. DIELECTRIC CONTINUUM THEORY OF SOLVATION DYNAMICS AND SPECTRAL DIFFUSION

The dielectric continuum theory has been widely utilized to describe solvation dynamics in dipolar solvents, such as methanol.[3,5–8] These electronic excited-state solvation dynamics as measured by TRF should be viewed as spectral diffusion with a Stokes shift driving force. The two following criteria must hold for dielectric continuum theory to accurately account for spectral diffusion dynamics:[3,5–8] (i) the change in the charge distribution following excitation needs to be the dominant perturbation and (ii) the long-distance response, the $k \rightarrow 0$ wave vector limit, of the surrounding solvent must dominate. For experiments utilizing electronic transitions to study solvation dynamics, theory and molecular-dynamics simulations have demonstrated the value of dielectric continuum model descriptions of spectral diffusion.[3,4,8] For experiments utilizing vibrational transitions, the results of this section indicate that the dielectric continuum model does not accurately describe the physical events that lead to spectral diffusion in the hydroxyl stretch of methanol-*d* dissolved in a solution of methanol-*h* and CCl_4.

The following model constitutes the simplest application of dielectric continuum theory. Even in this simple form, the theory has shown surprising success in describing a wide range of experimental measurements.[3,8] Within the framework of the dielectric continuum model, the reaction field represents the polarization of the solvent in response to the charge distribution of the solute, at the site of the solute.[9,34] Because optical absorption changes the charge distribution of the solute, the solvent reaction field will need to change to accommodate these changes in the solute.[9,34] Dielectric continuum theory attributes spectral diffusion to this time-dependent reaction field where the changes in the reaction field lie parallel to the change in the solute dipole moment because no perturbation exists perpendicular to the change in dipole.[9] For this reason, dielectric solvation dynamics reflect the longitudinal polarization relaxation of the solvent. The underlying physical process can be viewed as follows. The dipolar solvent molecules respond to the change in the solute dipole moment by reorienting their dipoles. This produces a change in the solvent generated reaction field felt by the solute, thus changing the solute-solvent interaction energy. This time-dependent solute-solvent interaction energy can be

monitored with transient vibrational hole burning via changes in the spectrum of the hole and excited-state stimulated emission.

The frequency-dependent dielectric constant $\varepsilon(\omega)$ of the solvent can be utilized to determine the long-wavelength solvent response, where $\varepsilon(\omega)$ contains the collective, time-dependent response of the solvent. Fourier–Laplace transformation provides both the transverse and the longitudinal collective dipole-dipole correlation functions:[8,9]

$$C_D^{(T)}(t)=\frac{\langle D_x(0)D_x(t)\rangle}{\langle D_x(0)^2\rangle}=[\varepsilon_0-\varepsilon_\infty]^{-1}\mathcal{L}_{i\omega}^{-1}(-[\varepsilon_0-\varepsilon(\omega)]/i\omega), \tag{14}$$

$$C_D^{(L)}(t)=\frac{\langle D_z(0)D_z(t)\rangle}{\langle D_z(0)^2\rangle}=\left[\frac{1}{\varepsilon_\infty}-\frac{1}{\varepsilon_0}\right]^{-1}\mathcal{L}_{i\omega}^{-1}\left(-\left[\frac{1}{\varepsilon(\omega)}-\frac{1}{\varepsilon_0}\right]\Big/\, i\omega\right), \tag{15}$$

where the superscripts T and L denote the transverse and longitudinal response, D_i the ith component of the time-dependent collective moment, ε_0 and ε_ω the zero and optical frequency dielectric constants, and $\mathcal{L}_{i\omega}^{-1}$ the inverse Fourier–Laplace transform. These collective dipole-dipole correlation functions can be calculated from the $\varepsilon(\omega)$ measured with dielectric relaxation experiments or terahertz spectroscopy.[9,35,36]

An alternative description of dipolar solvation dynamics that emphasizes the molecular orientational relaxation has been proposed.[8,37] In this description, the solvation dynamics can be expressed as a function of the ensemble averaged molecular dipole-dipole correlation function $C_\mu^{(1)}(t)$, where the superscript indicates this to be the correlation function for the first-order Legendre polynomial. $C_\mu^{(1)}(t)$ differs from $C_D^{(T)}(t)$ and $C_D^{(L)}(t)$, since $C_D^{(T)}(t)$ and $C_D^{(L)}(t)$ contain contributions from correlations between dipoles on different molecules, while $C_\mu^{(1)}(t)$ does not.[6,7,9] In the absence of intermolecular dipole correlations, $C_\mu^{(1)}(t)$ equals $C_D^{(T)}(t)$.[6,7,9] Computer simulations have indicated that the solvation dynamics result from two primary properties of the solvent:[37] the orientational relaxation dynamics as contained in $C_\mu(t)$ and the dipolar density,

$$\alpha_s \approx \frac{\rho\mu^2}{3\varepsilon k_B T}, \tag{16}$$

where ρ represents the solvent number density, μ the solvent dipole moment, ε the vacuum permittivity, k_B Boltzmann's constant, and T the absolute temperature. Simulations indicate that the solvation time correlation function $C_s(t)$ can be well represented by[37]

$$C_s(t)=[C_\mu^{(1)}(t)]^{\alpha_s}, \tag{17}$$

where methanol has an α_s of roughly 6.

We will now utilize Eqs. (14)–(17) and the orientational correlation function measured with time and polarization resolved pump-probe spectroscopy[13] to generate predicted spectral diffusion dynamics with which to compare to the experimental spectral diffusion. The dipole–dipole correlation function measured with polarization resolved pump-probe spectroscopy has a biexponential decay. The faster component has a 1.7 ± 0.7 ps time constant and accounts for $60\pm10\%$ of the relaxation, while the slower component decays with a 17 ± 3 ps time constant. This corresponds to a two component Debye model of the frequency-dependent dielectric constant $\varepsilon(\omega)$. Before calculating $\varepsilon(\omega)$, however, two distinctions between the orientational correlation function measured with polarization resolved pump-probe and dielectric relaxation experiments must be addressed. As mentioned previously, dielectric relaxation experiments measure a collective response while pump-probe experiments measure a molecular response.[9,38] Additionally, dielectric relaxation experiments measure the first-order Legendre polynomial orientational relaxation, while pump-probe experiments measure the second-order Legendre polynomial orientational relaxation.[9,13,38] The issues will now be discussed, before using the vibrational anisotropy data and Eqs. (14)–(17) to predict the time scales for spectral diffusion.

The work of Lipari and Szabo,[14] Wang and Pecora,[15] and Tokmakoff and Fayer[39] provide the necessary expressions for converting the observed $C_\mu^{(2)}(t)$ into $C_\mu^{(1)}(t)$. The resultant $C_\mu^{(1)}(t)$ also has a biexponential decay with decay times of 2 and 50 ps and a fast component amplitude of 27%.[13] The issue of collective versus molecular correlation functions have been discussed in detail in the literature.[7,9] As mentioned previously, the extent to which these functions differ depends on the extent to which the orientation of dipoles on different molecules correlate with one another. The collective dipole moment depends upon the ensemble averaged summation of all dipole correlations, $\langle\Sigma_{i,j}\mu_i\cdot\mu_j\rangle$, while only self correlations occur for the molecular correlation function, $i=j$.[7,9] The Kirkwood g factor provides a quantitative measure of these correlations, with a value of unity corresponding to no correlations. For hydrogen bonded liquids, intermolecular dipole correlations do occur with methanol having a g factor of 1.88.[40] While the importance of these correlations should not be dismissed, experiments appear to indicate that they do not significantly influence the observed dynamics. Pump-probe anisotropy measurements of $C_\mu^{(1)}(t)$ observed a slowest orientational relaxation time of $\sim$50 ps equal to the slowest relaxation times observed in dielectric relaxation and terahertz spectroscopy measurements of $C_D^{(T)}(t)$.[13,36] The decay of $C_\mu^{(1)}(t)$ and $C_D^{(T)}(t)$ have also been shown to be very similar for water.[36,41] We believe these strong similarities between $C_\mu^{(1)}(t)$ and $C_D^{(T)}(t)$ justify the use of $C_\mu^{(1)}(t)$ in Eq. (14). By taking the Fourier–Laplace transform of Eq. (14) we have been able to calculate $\varepsilon(\omega)$ from $C_\mu^{(1)}(t)$. We then utilized this $\varepsilon(\omega)$ in Eq. (15) to calculate $C_D^{(L)}(t)$, which provides a simple dielectric continuum theory prediction for solvation dynamics for a rigid solute chromophore.[34] An additional complication must also be addressed. For large dye molecule solutes, the orientational relaxation of the excited chromophores occurs much more slowly than the decay of $C_D^{(L)}(t)$. For the experiments being discussed in this paper, this will not be true, because a solvent molecule functions as the chromophore. Under these circumstances, the dielectric continuum theory predicts solvation dynamics equal to the

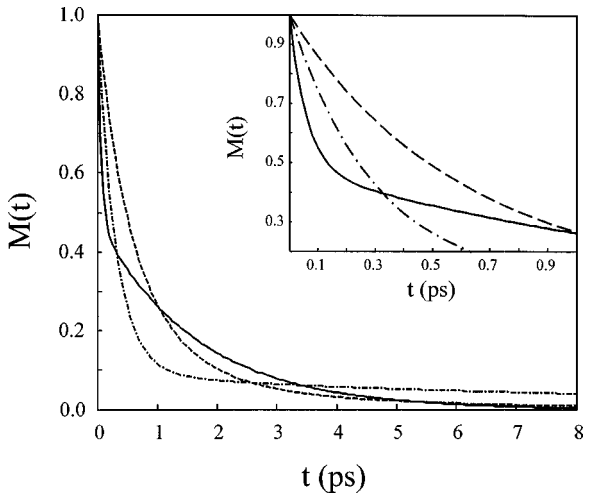

FIG. 7. Normalized solvation correlation functions as determined from the peak shift data (solid curve), the dielectric continuum model using $C_D^{(L)}(t)$ (dash-dot curve), and the polar solvation dynamics model $[C_\mu^{(1)}(t)]^{\alpha_s}$ (dash curve). Both models fail to describe the data.

product of the collective longitudinal relaxation and the molecular orientational relaxation:[34]

$$C_s(t) = C_D^{(L)}(t) C_\mu^{(1)}(t). \tag{18}$$

Equations (17) and (18) provide two different predictions for the spectral dynamics that have been observed with transient vibrational hole burning of the hydroxyl stretch of methanol-*d* dissolved in a solution of methanol-*h* and CCl_4. These appear in Fig. 7 along with the normalized experimental spectral diffusion dynamics $S(t)$ (solid curve). The normalized frequency–frequency correlation function parameters extracted from the experimental data with the model calculations discussed in Sec. IV can be found in Table II. These models [Eqs. (17) and (18)] that emphasize solvent polarization relaxation via molecular reorientation for spectral diffusion, do not accurately account for the experimental results. Two distinctions between the experimental data and the predicted dynamics warrant emphasis. First, the magnitude of the fast response in the predictions greatly exceeds the magnitude of the fast response in the experimental data. We emphasize that the limited time resolution of the experiment does not hamper our ability to accurately measure the magnitude of the fast response. This is because the difference in intensity of the pump laser pulse before and after it has traversed the sample provides an accurate account of the initial frequency of our signal maximum. Second, the slower relaxation component observed in the experiment decays much faster than the slower decays in the predictions. These model predictions appear to fail both in the amplitudes of the different relaxation processes as well as the time constants. While Fig. 7 clearly demonstrates models that emphasize the long-range collective orientational relaxation of the solvent do not accurately describe the measured dynamics, the source of these discrepancies constitutes the issue of particular significance.

The dielectric continuum model emphasizes the importance of the long-wavelength collective orientational response.[8,9] While the orientational correlation function we use to predict the dielectric continuum dynamics does not reflect the influence of intermolecular dipolar correlations, this does not appear to greatly influence the dynamics since the slow relaxation observed experimentally for the collective relaxation $C_D^{(T)}(t)$ does not differ from the molecular relaxation $C_\mu^{(1)}(t)$ observed experimentally.[13,36] An additional and more critical limitation in our application of dielectric continuum theory involves the role of carbon tetrachloride in the relaxation. The presence of CCl_4 in the solution means that the long-wavelength response of the solvent will not result solely from the response of the methanol molecules but also from the CCl_4. How this will influence the dielectric continuum relaxation remains unclear and cannot be ruled out as a potential source for the differences between the model predictions and the experimental results. While at present inconclusive, we believe the model fails to predict experimental data because the physical events embodied in the dielectric continuum approach do not correspond to the physical events that produce the experimental dynamics. We propose that spectral diffusion of the hydroxyl stretch depends predominantly on structural evolution in the local hydrogen bonding network rather than long-range collective orientational relaxation.[1,2,24] Recent simulations of hydroxyl stretch spectral diffusion in water provide support for this proposed explanation.[24] In these simulations, fast spectral diffusion on the 100 fs time scale results from coherently excited hydrogen bond translations, while the slower relaxation occurring on the ~1 ps time scale results from hydrogen bond dissociation. Should this physical picture hold for water and apply to methanol, the slower spectral diffusion time constant of 1.6 ps provides the average hydrogen bond lifetime. The 2.1 ps continuous hydrogen bond lifetime determined in molecular-dynamics simulations of methanol dissolved in CCl_4 further supports these conclusions.[21]

VI. CONCLUDING REMARKS

Frequency resolved pump-probe spectroscopy has been used to study hydroxyl stretch spectral diffusion in an isotopically mixed solution of methanol dissolved in CCl_4. We

TABLE II. Parameters used in the model calculations for Fig. 6.

Calculation	τ_r (ps)	$\tau_{d'}$ (ps)	$\tau_{d''}$ (ps)	$A_{d'}$ (amplitude)	$\nu_G(\infty)$ (cm^{-1})	$\Delta_G(\infty)=\Delta_{ES}(\infty)$ (cm^{-1})	Λ (cm^{-1})
a	0.5	0.06	1.6	0.52	2483.7	55	0
b	0.5	0.06	1.6	0.52	2483.7	55	3
c	0.5	0.06	1.6	0.52	2483.7	55	15

accessed these spectral diffusion dynamics by monitoring the time-dependent shift in the signal frequency maximum following the creation of a ground-state hole and excited-state peak on the high-frequency side of the doubly hydrogen bonded δ methanol-*d* band. The spectral diffusion dynamics have been fit to a bi-exponential, with time constants of $\sim$0.1 ps and 1.6 ± 0.3 ps with roughly equal amplitudes.

We conducted model calculations of frequency resolved pump-probe spectroscopy to extract the spectral diffusion dynamics. The calculations presented here differ from previous attempts in how they describe molecules in the hydroxyl stretch ground state that previously decayed from the excited state.[17,19,23] When the excited state decays to the ground state, the relaxation will occur vertically in the lower frequency modes of the solvent that produce spectral diffusion.[19] If the dynamics in the excited state differ from those in the ground state, the relaxed molecules will be characterized by a different absorption than the ground-state bleach at the moment of excited-state decay. Our model of frequency resolved pump-probe spectroscopy provides an appropriate treatment of these relaxed molecules, which we have termed antiholes, because they provide a vibrational ground-state signal with a sign opposite that of the ground-state hole. While antiholes have been ignored in theoretical descriptions of vibrational frequency resolved pump-probe experiments,[17,19,23] the potential significance of antiholes has been clearly demonstrated in persistent vibrational hole burning experiments.[33] A series of model calculations have been conducted to clarify the influence of antiholes on the frequency resolved pump-probe signal. These calculations demonstrate that antiholes make a significant contribution to the signal when the dynamics on the ground and excited state potential differ and the excited state decay and spectral diffusion occur with similar time constants. The proper treatment of antiholes could be of significance because excited-state decay and spectral diffusion occur on the same time scales for the hydroxyl stretch of hydrogen bonded liquids. Establishing the significance of antiholes on the signal will require identifying the differences between the dynamics in the ground and excited states. While the fit of the experimental peak position data presented in Fig. 6 used the same frequency–frequency correlation function in the ground and excited state and zero Stokes shift, the methyl rock overtone absorption on the low-energy side of the δ methanol-*d* absorption spectrum may hinder our ability to detect a Stokes shift. Although the significance of antiholes has yet to be established by experiment, any analysis that emphasizes the influence of a vibrational Stokes shift on the frequency resolved pump-probe signal[17,23] must explicitly account for the antihole signal.

We have used dielectric continuum theory[8,9] and the orientational relaxation dynamics of δ methanol-*d* measured with the hydroxyl stretch anisotropy decay[13] to make model predictions of the spectral diffusion dynamics. Within simple dielectric continuum theory, the longitudinal collective dipole-dipole correlation function determines the time scales for dipolar solvation dynamics.[8,9,34] The continuum theory,[8,9,34] and an additional model that emphasizes the orientational relaxation of the solvent,[8,37] fail to describe the observed spectral diffusion dynamics, indicating the long wavelength, collective orientational response does not provide the appropriate physical picture for the observed dynamics. We tentatively attribute the observed spectral diffusion of the hydroxyl stretch to structural evolution in the local hydrogen bonding network.[1,2,24] The same conclusions have been reached by recent simulations of hydroxyl stretch spectral diffusion in water.[24] In the water simulations, the 100 fs and $\sim$1 ps time scales of spectral diffusion reflect coherently excited hydrogen bond translations and hydrogen bond dissociation, respectively. By applying this physical picture of water to methanol, the slower spectral diffusion time constant of 1.6 ps provides the average hydrogen bond lifetime. The 2.1 ps continuous hydrogen bond lifetime determined in molecular-dynamics simulations of methanol dissolved in CCl_4 further supports these conclusions.[21]

The results obtained here on vibrational spectral diffusion should be contrasted with those obtained from the spectral diffusion dynamics of electronically excited dye molecules in a variety of solvents. A wide range of experimental and theoretical work has shown that dielectric continuum descriptions of solvation dynamics provide a reasonably accurate description of the electronic excited-state experimental data.[3,4,8] The experiments and theory have led to the conclusion that long-range orientational relaxation dominates the solvent response of large dielectric constant dipolar solvents. The inability of a simple continuum model to describe the spectral diffusion data for the hydroxyl stretch of methanol indicates that the vibrational dynamics experiments access a different aspect of the solvent response and may prove to be a sensitive monitor of local hydrogen bond dynamics.

ACKNOWLEDGMENTS

This work was supported by the Department of Energy (Grant No. DE-FG03-84ER13251), the National Science Foundation (DMR-0088942), the Air Force Office of Scientific Research (Grant No. F49620-01-1-0018), and the National Institutes of Health (IRO1-GM61137).

[1] O. Henri-Rousseau and P. Blaise, Adv. Chem. Phys. **103**, 1 (1998); S. Bratos and J. C. Leicknam, J. Chem. Phys. **101**, 4536 (1994).
[2] G. M. Gale, G. Gallot, F. Hache, N. Lascoux, S. Bratos, and J. C. Leicknam, Phys. Rev. Lett. **82**, 1068 (1999).
[3] M. L. Horng, J. A. Gardecki, A. Papazyan, and M. Maroncelli, J. Phys. Chem. **99**, 17 311 (1995).
[4] R. Biswas and B. Bagchi, J. Phys. Chem. B **101**, 2968 (1997); B. Bagchi and R. Biswas, Adv. Chem. Phys. **109**, 207 (1999).
[5] M. Maroncelli, J. Mol. Liq. **57**, 1 (1993).
[6] D. Kivelson and H. Friedman, J. Phys. Chem. **93**, 7026 (1989).
[7] P. Madden and D. Kivelson, Adv. Chem. Phys. **56**, 467 (1984).
[8] E. W. Castner and M. Maroncelli, J. Mol. Liq. **77**, 1 (1998).
[9] C. J. F. Böttcher, *Theory of Electric Polarization* (Elsevier, Amsterdam, 1973); C. J. F. Böttcher and P. Bordewijk, *Theory of Electric Polarization*, 2nd ed. (Elsevier, Amsterdam, 1978).
[10] P. V. Kumar and M. Maroncelli, J. Chem. Phys. **112**, 5370 (1999).
[11] K. Gaffney, I. Piletic, and M. D. Fayer, J. Phys. Chem. A **106**, 9428 (2002).
[12] K. J. Gaffney, P. H. Davis, I. R. Piletic, N. E. Levinger, and M. D. Fayer, J. Phys. Chem. A **106**, 12 012 (2002).
[13] K. J. Gaffney, I. R. Piletic, and M. D. Fayer, J. Chem. Phys. **118**, 2270 (2003).
[14] G. Lipari and A. Szabo, Biophys. J. **30**, 489 (1980); G. Lipari and A. Szabo, J. Am. Chem. Soc. **104**, 4546 (1982).
[15] C. C. Wang and R. Pecora, J. Chem. Phys. **72**, 5333 (1980).

[16] R. Laenen, C. Rausch, and A. Laubereau, Phys. Rev. Lett. **80**, 2622 (1998); R. Laenen and C. Rausch, J. Chem. Phys. **106**, 8974 (1997).
[17] S. Woutersen and H. J. Bakker, Phys. Rev. Lett. **83**, 2077 (1999).
[18] M. Berg, C. A. Walsh, L. R. Narasimhan, K. A. Littau, and M. D. Fayer, J. Chem. Phys. **88**, 1564 (1988); K. A. Littau, Y. S. Bai, and M. D. Fayer, Chem. Phys. Lett. **159**, 1 (1989); K. A. Littau, M. A. Dugan, S. Chen, and M. D. Fayer, J. Chem. Phys. **96**, 3484 (1992); M. Bonn, M. J. P. Brugmans, A. W. Kleyn, R. A. van Santen, and H. J. Bakker, *ibid.* **105**, 3431 (1996).
[19] S. Mukamel, *Principles of Nonlinear Optical Spectroscopy* (Oxford University Press, New York, 1995).
[20] H. Graener, T. Q. Ye, and A. Laubereau, J. Chem. Phys. **91**, 1043 (1989); O. Kristiansson, J. Mol. Struct. **477**, 105 (1999); U. Liddel and E. D. Becker, Spectrochim. Acta **10**, 70 (1957); A. Staib, J. Chem. Phys. **108**, 4554 (1998); M. C. R. Symons and V. K. Thomas, J. Chem. Soc., Faraday Trans. **77**, 1883 (1981); D. M. zum Buschenfelde and A. Staib, Chem. Phys. **236**, 253 (1998).
[21] R. Veldhuizen and S. W. de Leeuw, J. Chem. Phys. **105**, 2828 (1996).
[22] J. E. Bertie and S. L. Zhang, J. Mol. Struct. **413–414**, 333 (1997).
[23] M. F. Kropman and H. J. Bakker, Science **291**, 2118 (2001); M. F. Kropman and H. J. Bakker, J. Chem. Phys. **115**, 8942 (2001); M. F. Kropman, H.-K. Nienhuys, S. Woutersen, and H. J. Bakker, J. Phys. Chem. A **105**, 4622 (2001).
[24] R. Rey, K. B. Møller, and J. T. Hynes, J. Phys. Chem. A **106**, 11 993 (2002); C. P. Lawrence and J. L. Skinner, Chem. Phys. Lett. **369**, 472 (2003); M. Diraison, Y. Guissani, J. C. Leicknam, and S. Bratos, *ibid.* **258**, 348 (1996).
[25] J. R. Kuppers, J. Electrochem. Soc. **125**, 97 (1978).
[26] C. P. Lawrence and J. L. Skinner, J. Chem. Phys. **117**, 8847 (2002).
[27] R. Laenen, G. M. Gale, and N. Lascoux, J. Phys. Chem. A **103**, 10 708 (1999).
[28] L. K. Iwaki and D. D. Dlott, J. Phys. Chem. A **104**, 9101 (2000).
[29] S. L. Palfrey and T. F. Heinz, J. Opt. Soc. Am. B **2**, 674 (1985).
[30] M. D. Fayer, *Elements of Quantum Mechanics* (Oxford, New York, 2001).
[31] L. D. Landau and E. M. Lifshitz, *Statistical Physics, Part I* (Pergamon, New York, 1980).
[32] T. Fonseca and B. M. Ladanyi, J. Phys. Chem. **95**, 2116 (1991); L. Turi, P. Minary, and P. J. Rossky, Chem. Phys. Lett. **316**, 465 (2000).
[33] H. L. Strauss, Acc. Chem. Res. **30**, 37 (1997).
[34] B. Bagchi, D. W. Oxtoby, and G. R. Fleming, Chem. Phys. **86**, 257 (1984).
[35] R. Buchner and J. Barthel, J. Mol. Liq. **52**, 131 (1992).
[36] J. Barthel, K. Bachhuber, R. Buchner, and H. Hetzenauer, Chem. Phys. Lett. **165**, 369 (1990); J. T. Kindt and C. A. Schmuttenmaer, J. Phys. Chem. **100**, 10 373 (1996).
[37] M. Maroncelli, P. V. Kumar, and A. Papazyan, J. Phys. Chem. **97**, 13 (1993).
[38] B. J. Berne and R. Pecora, *Dynamic Light Scattering* (Wiley, New York, 1976).
[39] A. Tokmakoff and M. D. Fayer, J. Chem. Phys. **103**, 2810 (1995).
[40] W. H. Orttung, T. H. C. Sun, and J. M. Kim, J. Phys. Chem. **97**, 5392 (1993).
[41] C. Rønne, P.-O. Åstrand, and S. R. Keiding, Phys. Rev. Lett. **82**, 2888 (1999); H.-K. Nienhuys, R. A. van Santen, and H. J. Bakker, J. Chem. Phys. **112**, 8487 (2000).